Three Dimensional Fracture Material Model for Ultra-high Performance Fiber Reinforced Concrete under Tensile Loading

Man Xu[1], Kay Wille[1]
[1]Department of Civil & Environmental Engineering, University of Connecticut, USA, 06269

Abstract:

Ultra-high performance fiber reinforced concrete (UHP-FRC) can be designed to exhibit strain hardening response under tensile loading accompanied by multiple cracks and relatively large energy absorption prior to fracture localization. However, existing material models in the finite element code are challenged to capture such strain hardening and multiple cracking behaviors. Therefore, a three dimensional fracture material model based on smeared rotating/fixed crack theory is developed to accurately represent the tensile behavior of UHP-FRC. In the proposed fracture material model, Rankine yield surface is used to govern the crack initiation and the proposed shape of the tensile-softening diagram for UHP-FRC is used to control the crack propagation. Crack band-width approach is used to guarantee the mesh objectivity. The proposed fracture material model for UHP-FRC is successfully implemented and compiled in LS-DYNA through the UMAT (User MATerial Subroutine). The numerical simulation of uniaxial tension test is conducted to validate the developed material model and the results reveal that the developed fracture material model shows an agreement with the test data and is capable to capture the behaviors of strain hardening, multiple cracking and softening of UHP-FRC under tensile loading.

Keywords: smeared crack theory, fracture model, UHP-FRC, strain hardening, finite element analysis

1. Introduction

Ultra-high performance fiber reinforced concrete (UHP-FRC) has attracted the growing interest of many researchers, engineers and contractors across the world due to its highly enhanced strength, ductility, shear resistance, energy dissipation capacity, and damage tolerance in comparison to normal strength concrete (NSC) [1-6]. With respect to the tension behavior of UHP-FRC, a key characteristic is that UHP-FRC exhibits strain hardening response accompanied by multiple cracks and thus relatively large energy absorption prior to fracture localization [4-6].

Nowadays, numerical simulation has been approved as an effective way to predict the material behavior. In order to predict with high accuracy the tensile behavior of UHP-FRC, appropriate constitutive models must be used. Nevertheless, existing material model in the finite element code are challenged of capturing the tensile responses of UHP-FRC, especially strain-hardening (multiple cracking) and softening (failure crack opening) behavior. Therefore, in this paper a three dimensional material fracture model for UHP-FRC is developed to accurately represent the tensile behavior, such as strain hardening, cracking, and softening responses. The proposed fracture model is based on the smeared crack theory developed by J. G. Rots and modified to represent the whole fracture process of UHP-FRC from strain hardening to

softening. Rotating/ fixed method is applied to control the orientation of the crack and crack band-width method is adopted to assure the mesh objectivity.

2. Background

J. G. Rots [7] developed the smeared crack theory for concrete fracture, with the cracked solid imagined to be a continuum, and use an orthotropic stress-strain law upon crack formation.

The constitutive relation between incremental global stress ($\Delta\sigma$) and incremental global strain ($\Delta\varepsilon$) can be written as:

$$\Delta\sigma = [D^e - D^e N[D^{cr} + N^T D^e N]^{-1} N^T D^e]\Delta\varepsilon \tag{1}$$

D^e is the elastic modulus matrix of UHP-FRC. N is called the transformation matrix reflecting the direction of the crack plane and defined as

$$N = \begin{bmatrix} l_x^2 & l_x l_y & l_z l_x \\ m_x^2 & m_x m_y & m_z m_x \\ n_x^2 & n_x n_y & n_z n_x \\ 2l_x m_x & l_x m_y + l_y m_x & l_z m_x + l_x m_z \\ 2m_x n_x & m_x n_y + m_y n_x & m_z n_x + m_x n_z \\ 2n_x l_x & n_x l_y + n_y l_x & n_z l_x + n_x l_z \end{bmatrix} \tag{2}$$

Where l_x, m_x, n_x form a vector defining the direction of the normal crack, l_y, m_y, n_y, and l_z, m_z, n_z form the two vectors defining the orientations of two shear cracks in the global coordinate system. N^T is the transpose matrix of N.

D^{cr}, the crack constitutive matrix, is diagonal and composed of mode I, mode II, and mode III stiffness modulus associated with the crack behavior. D^{cr} is defined as

$$D^{cr} = \begin{bmatrix} D_I^{cr} & 0 & 0 \\ 0 & D_{II}^{cr} & 0 \\ 0 & 0 & D_{III}^{cr} \end{bmatrix} \tag{3}$$

3. Proposed Fracture Model

The proposed three dimensional fracture model for UHP-FRC is based on the aforementioned smeared crack theory developed by J.G. Rots. We extend Rots's stress-strain formula of strain softening stage to the whole fracture stage including strain hardening and softening.

The crack initiation in the present model is governed by the Rankine yield surface, which is that when the maximum principal stress, σ_1, exceeds the uniaxial tensile strength, f_t , a crack is formed. After crack occurring, the crack propagation is controlled by the shape of the normal crack stress-strain diagram and the material fracture energy. The proposed combined linear and exponential normal crack stress-strain diagram [8] is illustrated in **Figure 1** and defined by

$$\sigma_n^{cr} = \begin{cases} \sigma_{tc} + D_{I,1}^{cr}\varepsilon_n^{cr} & 0 < \varepsilon_n^{cr} \le \beta\varepsilon_{n,ult}^{cr} \\ \sigma_{tp}\left[\left[1 + \left(C_1 \frac{(\varepsilon_n^{cr} - \beta\varepsilon_{n,ult}^{cr})}{\varepsilon_{n,ult}^{cr}}\right)^3\right]\exp\left(-C_2 \frac{(\varepsilon_n^{cr} - \beta\varepsilon_{n,ult}^{cr})}{\varepsilon_{n,ult}^{cr}}\right) - \frac{(\varepsilon_n^{cr} - \beta\varepsilon_{n,ult}^{cr})}{\varepsilon_{n,ult}^{cr}}\left(1 + {C_1}^3\right)\exp(-C_2)\right] & \beta\varepsilon_{n,ult}^{cr} < \varepsilon_n^{cr} < \varepsilon_{n,ult}^{cr} \\ 0 & \varepsilon_n^{cr} \ge \varepsilon_{n,ult}^{cr} \end{cases} \tag{4}$$

Where σ_n^{cr} and ε_n^{cr} are the normal crack stress and normal crack strain, respectively. σ_{tc} and σ_{tp} are the cracking stress and peak stress under uniaxial tension, respectively. C_1 and C_2 are material parameters controlling the exponential shape of normal crack stress-strain diagram. β is the parameter defining the percentage of fracture energy generated during strain hardening stage. And the ultimate normal crack strain, $\varepsilon_{n,ult}^{cr}$, is obtained from

$$\varepsilon_{n,ult}^{cr} = l_f/(2h) \tag{5}$$

Where l_f is the fiber length, and h is the crack band-width.

The model I, model II and model III crack stiffness modulus are calculated by:

$$D_{I,1}^{cr} = \frac{(\sigma_{tp}-\sigma_{tc})}{\beta\varepsilon_{n,ult}^{cr}} \tag{6}$$

$$D_{I,2}^{cr} = \sigma_{tp}\left[\exp\left(-C_2\frac{(\varepsilon_n^{cr}-\beta\varepsilon_{n,ult}^{cr})}{\varepsilon_{n,ult}^{cr}}\right)\left[-\frac{C_2}{\varepsilon_{n,ult}^{cr}}-\frac{C_2}{\varepsilon_{n,ult}^{cr}}\left(C_1\frac{(\varepsilon_n^{cr}-\beta\varepsilon_{n,ult}^{cr})}{\varepsilon_{n,ult}^{cr}}\right)^3+3\frac{{C_1}^3}{\varepsilon_{n,ult}^{cr}}\left(\frac{\varepsilon_n^{cr}-\beta\varepsilon_{n,ult}^{cr}}{\varepsilon_{n,ult}^{cr}}\right)^2\right]-\frac{1}{\varepsilon_{n,ult}^{cr}}\left(1+{C_1}^3\right)\exp(-C_2)\right] \tag{7}$$

$$D_{II}^{cr} = D_{III}^{cr} = \frac{(1-\frac{\varepsilon_n^{cr}}{\varepsilon_{n,ult}^{cr}})^p}{1-(1-\frac{\varepsilon_n^{cr}}{\varepsilon_{n,ult}^{cr}})^p}G \tag{8}$$

Where G is the shear modulus.

Mesh objectivity is a necessity in the finite element analysis of softening behavior. In the proposed fracture model, the crack band width approach is used to guarantee the mesh objectivity. Based on the smeared crack approach, the fracture zone is regarded to spread over in a certain width of the finite element, which is called crack band width, h.

In order to accurately represent the crack orientation during the fracture process, the rotating/fixed method for the crack direction is employed in this paper. Once the crack is initiated, it can change direction arbitrarily until crack localization occurs. After localization, the crack direction is fixed.

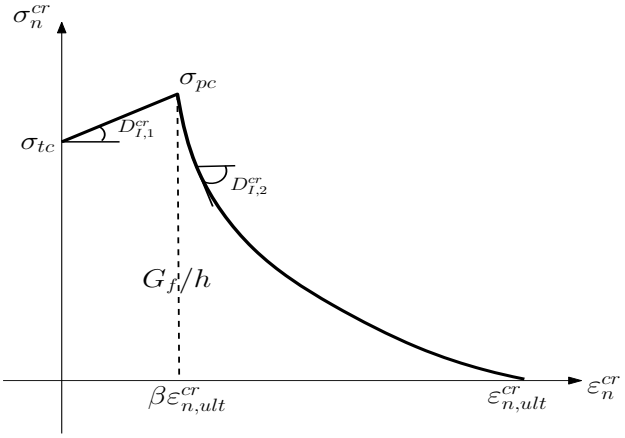

Figure 1. Proposed linear and exponential normal crack stress-strain diagram

4. Implementation in LS-DYNA

The proposed fracture model is compiled with FORTRAN and implemented in LS-DYNA as a user-defined material subroutine called UMAT. The executable file is generated within the UMAT and linked to LS-DYNA as a new solver (**Figure 2**). At each time step, the incremental strain ($\Delta\varepsilon$), the previous state of stress (σ^{m-1}) and strains (ε^{m-1}), and the history variables from the main program are treated as inputs and passed to UMAT for integration. The outputs from UMAT are the current state of stresses (σ^{m}) and strains (ε^{m}), and updated history variables which are needed for the next time step.

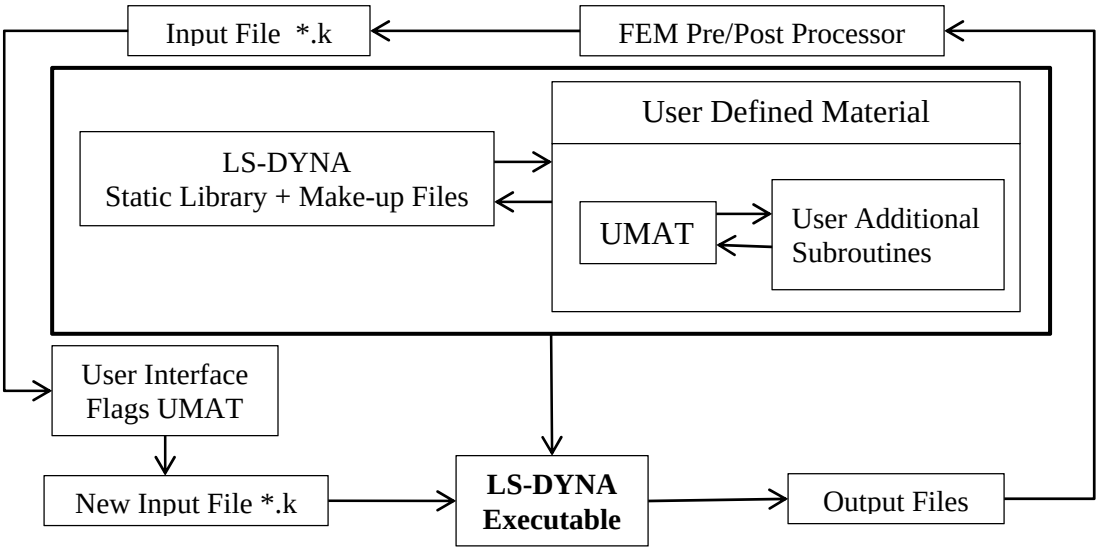

Figure 2. Configuration of the UMAT in LS-DYNA [9]

5. Model Verification

5.1. Identification of Material Parameters

For the proposed fracture model, a total of 12 material parameters are required to define the constitutive equation and normal crack stress-strain relationship. The 12 parameters are obtained from uniaxial tensile test for UHP-FRC [4] and shown in **Table 1**.

Table 1 Material Parameters for the Fracture Model

E_c (MPa)	ν	σ_{tc} (MPa)	ε_{tc}	σ_{tp} (MPa)	ε_{tp}
56000	0.2	11.8	0.000211	15.1	0.00488
G (MPa)	β	C_1	C_2	G_f (MPa/mm)	l_f (mm)
23333	0.006	3.0	5.93	20	13

5.2. Results and Discussion

The first exercise to ensure that the proposed fracture model works is to simulate a single three-dimensional solid element subjected to uniaxial and triaxial tension loadings. A fully integrated solid element with the dimension of 1x1x1 inch is used and a prescribed displacement is specified at nodal points. In the uniaxial loading case, the prescribed displacement is applied at node on the top face. In the triaxial case, besides the displacement control at the top surface nodes, two different confining pressures are applied to demonstrate their effect on the strength

and ductility of the material. In the triaxial case, the two chosen confining pressure levels are -2 MPa (tension) and 2 MPa (compression). Proposed fracture model is assigned as material model for the single element. The computed stress strain responses under uniaxial and triaxial tension are plotted in **Figure 3**. From the curves shown in **Figure 3**, it is concluded that the strength and its corresponding strain are dependent upon the confining pressure. Decreasing the confining pressure will reduce the strength and ductility.

After the single element simulation has been verified, numerical simulation of uniaxial tension of a dog-bone UHP-FRC specimen with the dimension of 1x1x3 inch (gauge length) is being performed using the proposed fracture material model. A quarter of the whole specimen is adopted in the simulation and corresponding boundary conditions are assigned. The axial tensile force is applied by displacement control on the top face. **Figure 4** shows the comparison of the stress versus strain curves from test [4] and simulations. The results indicates that the simulation stress strain curve agrees well with the test stress strain curve and suggests that the fracture model is able to characterize the strain-hardening and softening behaviors of UHP-FRC under tension loadings.

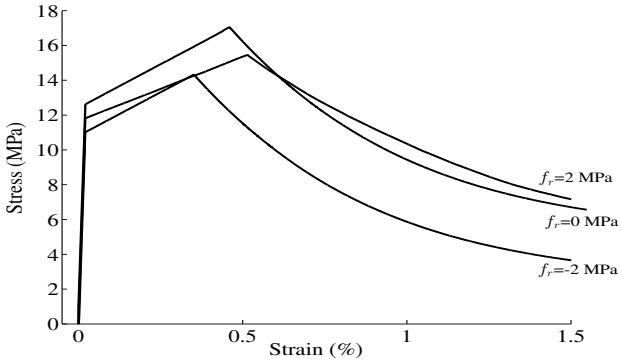

Figure 3. Uniaxial and triaxial tension of one element

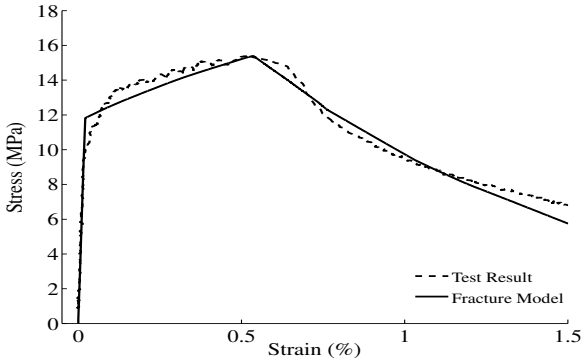

Figure 4. Comparison of test result and simulation under uniaxial tension

Figure 5 illustrates the contours of the principal strain of specimen at various loading stages under uniaxial tensile loading. **Figure 5 (a)** shows the principal strain just after ε_{tc} (cracking strain) and the multiple hairline cracking occur. When the principle strain is increasing to ε_{tp} (strain at peak stress), the multiple cracking becomes more pronounced and crack localization is just initiated (see **Figure 5 (b)**). As the principle strain is further increasing, its corresponding contour in **Figure 5 (c)** indicates that crack localization accompanied by multiple cracking has become more significant. **Figure 5** demonstrates that the proposed fracture model is able of capturing the multiple cracking behavior during strain hardening regime and crack localization during softening regime of UHP-FRC.

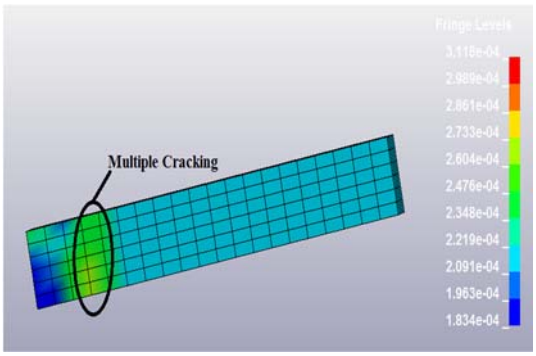

(a) Initiation of multiple cracking

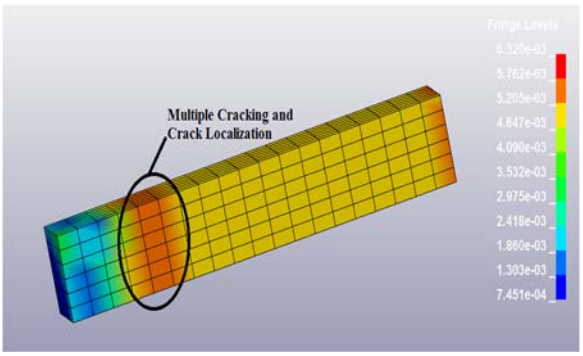

(b) Initiation of crack localization

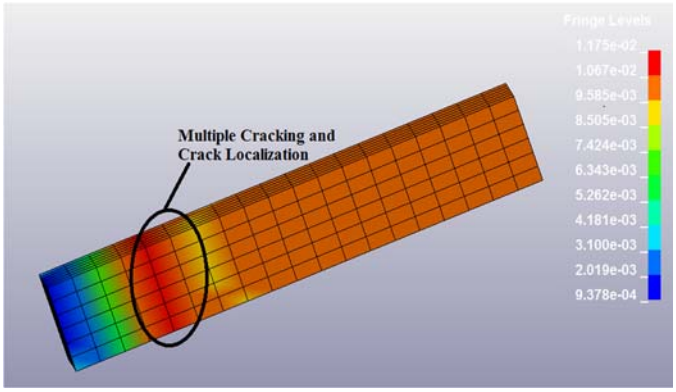

(c) Crack localization accompanied by multiple cracking

Figure 5. Contour plots of the principal strain

6. Conclusion

Motivated by the limitation of finite element material models to represent UHP-FRC tensile behavior including strain hardening and softening response, a three dimensional fracture material model is proposed to capture the tensile behavior of UHP-FRC. The proposed fracture model is based on the smeared crack theory and modified to represent the whole fracture stage including strain hardening and softening of UHP-FRC under tensile loading. Rankine yield surface, crack band width method, and rotating/fixed crack direction approach are adopted in the model. Within UMAT in LS-DYNA the material model is successfully implemented as the material subroutine for numerical simulation. The comparison of the simulation result and test data of UHP-FRC under uniaxial tension demonstrates that the proposed fracture model is able to predict the behavior of UHP-FRC with satisfactory accuracy in terms of strength, strain hardening behavior, and softening behavior. Moreover, the multiple cracking during strain hardening stage and crack localization during softening stage can be captured by the proposed fracture model.

7. Reference

[1] Wille K, Naaman AE, El-Tawil S, Parra-Montesinos GJ, "Ultra-high Performance Concrete and Fiber Reinforced Concrete: Achieving Strength and Ductility Without Heat Treatment". Materials and Structures 45(3):309–324, 2012.
[2] Wille K, Naaman AE, Parra-Montesinos GJ, "Ultra High Performance Concrete with Compressive Strength Exceeding 150 MPa (22kis): A Simpler Way". ACI Material Journal, 1: 46–54, 2012
[3] Wille K, Naaman AE, El-Tawil S, "Ultra High Performance Fiber Reinforced Concrete (UHP-FRC) Record Performance under Tensile Loading". Concrete International, 33(9): 35–41, 2011.
[4] Wille K, El-Tawil S, Naaman AE, "Properties of Strain Hardening Ultra High Performance Fiber Reinforced Concrete (UHP-FRC) under Direct Tensile Loading". Cement and Concrete Composites, 48: 53–66, 2014.
[5] Xu, M., Wille, K., "Fracture Energy of UHP-FRC under Direct Tensile Loading Applied at Low Strain Rates", Elsevier – Composites Part B: Engineering Journal. Vol. 80. 2015. pp. 116 – 125.
[6] Wille, K., Xu, M., El-Tawil, S., Naaman, A.E. "Dynamic Impact Factors of Strain Hardening UHP-FRC under Direct Tensile Loading at Low Strain Rates," Materials and Structures, published online March 07, 2015.
[7] Rots, J.G. "Computational Modeling of Concrete Fracture." PhD Thesis, Delft University of Technology, The Netherlands, 1988.
[8] Reinhardt, H., Cornelissen, H., and Hordijk, D. "Tensile Tests and Failure Analysis of Concrete." Journal of Structural Engineering, 112(11), 2462–2477, 1986.
[9] Moraes and Nicholson, "Simulation of Projectile Impact using Continuum Damage Mechanics", ASME Pressure Vessels and Piping Conference, 39-46, 2001.

8. Acknowledge

The authors would like to thank the Schlumberger Foundation for their financial support of this research project.